Int J Adv Manuf Technol (2014) 72:475–485
DOI 10.1007/s00170-014-5691-0

ORIGINAL ARTICLE

Cutting performance of an indexable insert drill for difficult-to-cut materials under supplied oil mist

Masato Okada · Naoki Asakawa · Eisuke Sentoku · Rachid M'Saoubi · Takashi Ueda

Received: 24 October 2013 / Accepted: 4 February 2014 / Published online: 19 February 2014

Abstract In this study, the cutting performance of an indexable insert drill with an asymmetric geometry for cutting difficult-to-cut materials was investigated. A solid twist drill with a symmetric geometry was used to compare the cutting characteristics. The cutting characteristics were evaluated using the thrust force, inner-surface roughness of the drilled hole, wear behavior, and tool temperature. Workpieces made of stainless steel, titanium alloy, and nickel-based alloy were selected as difficult-to-cut materials, and carbon steel was also selected. The tool temperature was higher in the order of carbon steel, stainless steel, titanium alloy, and nickel-based alloy for every drill under minimum quantity lubrication cutting. The influence of the workpiece material on the thrust force was different from that of the tool temperature for the indexable insert drill, whereas that of the solid twist drill was similar to the tool temperature tendency. When cutting the titanium alloy and nickel-based alloy, the tool temperature and thrust force of the indexable insert drill were lower than those of the solid-type twist drill. The inner-surface roughness of a hole drilled with the indexable insert drill had almost the same quality as that of a hole drilled with the solid-type twist drill when cutting the difficult-to-cut materials. The wear behavior of the indexable insert drill was remarkably different from that of the solid-type twist drill, and the flaking of the coating and the abrasion wear at the rake face were notable in the indexable insert drill.

Keywords Drilling · Indexable insert drill · Difficult-to-cut materials · Tool temperature · Tool wear · Minimum quantity lubrication

M. Okada (✉) · N. Asakawa · T. Ueda
Institute of Science and Engineering, Kanazawa University, Kakuma-machi, Kanazawa, Ishikawa 920-1192, Japan
e-mail: okada@se.kanazawa-u.ac.jp

E. Sentoku
Department of Mechanical Engineering, Fukui National College of Technology, Geshi-cho, Sabae, Fukui 916-8507, Japan

R. M'Saoubi
SECO TOOLS AB, Fagersta 73782, Sweden

Abbreviations

BEI	Backscattered electron image
I718	Inconel 718 (nickel-based alloy)
MR	Machinability rating
SEM	Scanning electron microscope
Ti64	Ti–6Al–4V (titanium α+β alloy)
1045	AISI 1045 (carbon steel)
304	AISI 304 (austenitic stainless steel)
D	Drill diameter (mm)
D_p	Prepared hole diameter (mm)
f	Feed rate (mm/rev)
f_z	Feed per tooth (mm/tooth)
F_t	Thrust force (N)
L_c	Cutting length (m)
L_d	Effective length of drill (mm)
p	Supply pressure of compressed air (MPa)
q	Flow rate of oil mist (ml/h)
Ra	Arithmetic average roughness of finished surface (μm)
v_c	Cutting speed (m/min)
VB_o	Bottom flank wear of outer insert (μm)
w_c	Chamfer width (mm)
α	Point angle of drill (°)
ϕ	Measuring area diameter of temperature (μm)
θ_α	Peripheral corner edge temperature (°C)
γ	Rake angle of drill (°)
ψ_c	Chamfer angle (°)

ξ Back taper angle of drill (°)
ζ Relief angle of drill (°)

1 Introduction

Drilling tools have been used in the majority of hole-making processes in industry. Therefore, many studies have been performed to improve the cutting performance and develop a better drill geometry. Ultrasonic-assisted drilling is a typical cutting method that is used to improve the cutting performance. Neugebauer and Stoll [1] evaluated the effect of using ultrasonic-assisted drilling for aluminum alloys in terms of cutting force reduction and chip removal. On the other hand, in a study on drill geometry, Lazar and Xirouchaks [2] theoretically dealt with the mechanical load distribution along the main cutting edge during drilling and experimentally evaluated the most appropriate drill geometry for cutting composite materials. Audy [3] proposed a method for predicting the cutting force during drilling using a computer and clarified the influence of drill geometry characteristics such as the chisel edge and the rake angle distributions along the drill lips on the thrust force and cutting torque. Lin [4] reported the experimental cutting performance of a coated carbide drill with a curved cutting edge used for stainless steel. Many of these studies targeted a solid-type twist drill (solid drill), which has a chisel edge at the point, a point angle of 120–140°, and an axial symmetric geometry, because it is commonly used to make holes in various materials in industry. Various drills with geometries that differ from that of a solid drill have also been developed, and their cutting characteristics have been investigated. Tsao and Hocheng [5] reported the effects of different drill geometries, such as a saw drill, candle stick drill, and core drill, on the delamination of composite materials. Zhao and Ehmann [6] also analyzed the performance of a spade drill bit. On the other hand, indexable insert drills (indexable drills) have been developed, which have multiple indexable inserts and an asymmetric geometry. Indexable drills consist of two inserts with different shapes and a reusable holder. These have the advantages of making possible a fine adjustment of the hole diameter and easy drill changes. In particular, an indexable drill is relatively inexpensive compared with a solid drill because regrinding, recoating, and spare tools are unnecessary, which very effectively improves the productivity. The authors have already investigated the cutting characteristics of indexable drills used for cutting carbon steel [7]. Venkatesh and Xue [8] clarified the influence of the built-up edge on the surface roughness with an indexable drill used for cutting low-carbon steel. Venkatesh et al. [9] also reported the influence of the drill geometry on the cutting force in the same material. Wang et al. [10] proposed an improved indexable drill for finishing in the cutting of AISI 1026. However, the cutting performance of an indexable drill when cutting difficult-to-cut materials has not been clarified. In particular, the tool temperature, which has an extremely large influence on the tool life and hole quality, during cutting with an indexable drill has not been clarified, whereas various studies on the tool temperature during drilling of difficult-to-cut materials with a conventional twist drill have been reported. For instance, Li and Shih [11] reported an experimental and analytical evaluation of the tool temperature when drilling a titanium alloy using a conventional twist drill. Zeilmann and Weingaertner [12] also reported the influence of the cutting condition on the tool temperature during the drilling of a titanium alloy with a conventional twist drill.

In this study, the cutting characteristics of an indexable drill used for cutting difficult-to-cut materials under a supplied oil mist (minimum quantity lubrication (MQL)) were investigated experimentally by comparing them with those of a solid drill. MQL was a significant factor in reducing the energy for the circulation of the lubrication oil, simplifying the production cleaning process, and improving the work environment, because it could remarkably reduce the consumption of the lubrication oil. In particular, MQL is expected to be effective in the cutting of difficult-to-cut materials, which are difficult to dry cut, and various investigations have been performed relating to MQL [12]. The cutting characteristics were mainly evaluated using the peripheral cutting edge temperature, thrust force, inner-surface roughness, and tool wear behavior. Stainless steel, titanium alloy, and nickel-based alloy were used as the difficult-to-cut materials, and carbon steel was used to compare the influences of the material properties. The influences of the cutting speed and feed rate on the tool temperature and thrust force in drilling of the titanium alloy were also investigated.

2 Experimental method

2.1 Indexable insert drill

Pictures of the indexable and solid drills and a schematic illustration of the indexable drill used in this study are shown in Figs. 1 and 2, respectively. In the case of the indexable drill, the inner and outer inserts, which had different geometries, were fixed on the reusable insert holder using a locking screw. The inserts were fixed at different distances from the rotational axis, and the lengths of the bottom cutting edges of both inserts were shorter than the radius of the drilled hole. Therefore, each insert cut separately at the center side and outside of the drilled hole, and the cutting areas of the inserts were limited to a small area, as shown in Fig. 3. Therefore, the geometry of an indexable drill is substantially different from that of a solid drill, which has two cutting edges with the same shape. Consequently, the feed rate per tool rotation became the

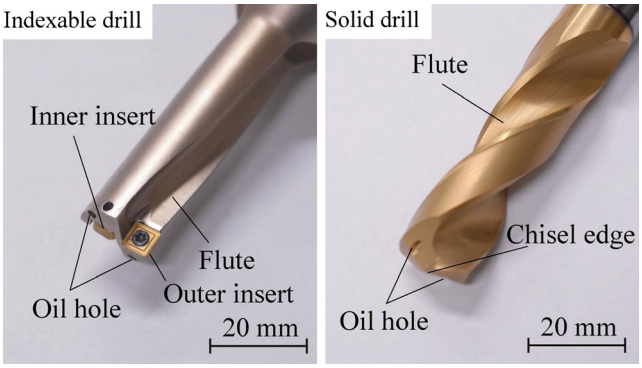

Fig. 1 Pictures of indexable insert and solid-type twist drill

feed per tooth for the indexable drill, whereas half of the feed rate per tool rotation became the feed per tooth for the solid drill. The inner and outer inserts were inclined from the rotational axis by 1.0° and 2.5°, respectively, and the corner angles of the inserts were all 90°. Thus, the back taper angle of the indexable drill became ξ=2.5°, whereas that for the solid drill used in this investigation was approximately ξ=0.15°. Moreover, the point angle of the indexable drill was approximately 2α=180°, which was much larger than for the solid drill, which was 2α=140°. The detailed geometry of the outer insert is shown in Fig. 4. As seen in this figure, the outer insert had a chip breaker on the rake face and a land with a 0.12-mm width and 0° at the cutting edge. The relief angle of the outer insert at the bottom and peripheral corner was 7°, and the outer insert did not have the margin area. In addition, the base material of the cemented carbide tool was coated with multiple layers of (Ti,Al)N+TiN using the PVD method.

2.2 Two-color pyrometer

It is difficult to measure the cutting edge temperature during drilling, because the drill rotates and feeds at high speed within the workpiece, and the area to be measured is very small. Therefore, a two-color pyrometer with an optical fiber was used as a noncontact thermometer in this experiment. This pyrometer had a flat response up to approximately 100 kHz and a small measuring area diameter of approximately ϕ=500 μm. A schematic illustration of the two-color pyrometer is shown in Fig. 5. The infrared rays from the object were captured by a chalcogenide glass fiber and fed to the two-color detector. The two-color detector incorporated an InAs photodetector mounted over an InSb photodetector along the same optical axis. The InAs detector responded to incident radiation from 1.0 to 3.0 μm and transmitted waves larger than 3.0 μm, and the InSb detector responded to radiation from 3.0 to 5.5 μm. The infrared energy was converted into an amplified electric signal. By obtaining the ratio of the output voltages from the two detectors, we could calculate the temperature of the object using the calibration curve obtained by sighting the incidence face of the optical fiber on a radiating surface of known uniform temperature. Additionally, the ratio of the outputs from the two-color detector made it possible to cancel small disturbances such as those from changes of the surface quality of the cutting edge during drilling. Thus, this pyrometer can measure the cutting edge temperature without the influence of emissivity. The authors had previously used this pyrometer to investigate the thermal phenomena in various processes such as end milling [13] and turning [14]. It had already been confirmed that temperature measurement during MQL cutting was possible using this pyrometer type [15].

2.3 Temperature measurement

Figure 6 shows schematic illustrations of the workpiece geometry and experimental arrangement for temperature measurements during drilling. The temperature at the corner edge of the outer insert during cutting was measured. An optical fiber was inserted into the slot from the outer surface of the workpiece. The optical fiber was fixed in the slot at the point where the distance between the corner edge of the outer insert and the incidence face of the optical fiber was 0.5 mm. The optical fiber could capture the infrared energy radiated from the peripheral corner edge of the drill when it passed above the slot. The authors clarified that the outer corner edge had the

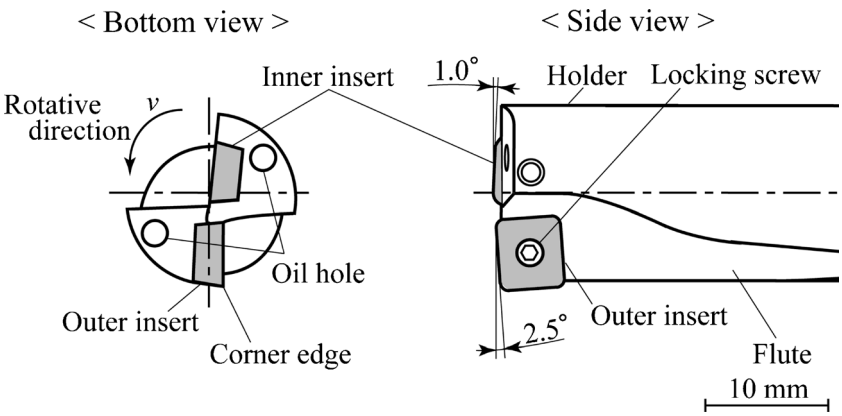

Fig. 2 Schematic illustration of indexable insert drill

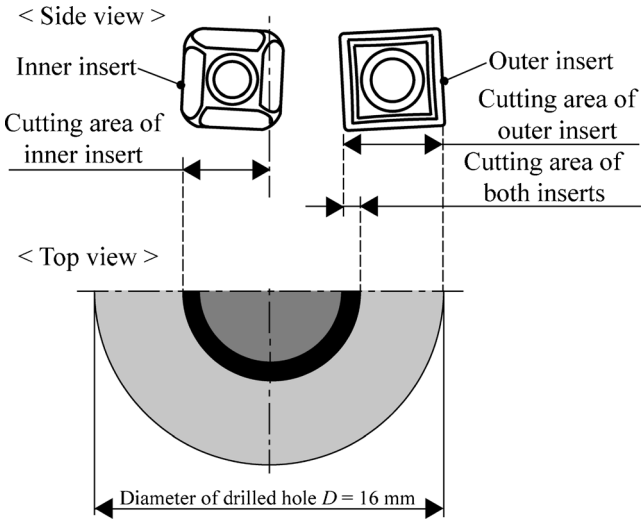

Fig. 3 Cutting areas of inner and outer inserts

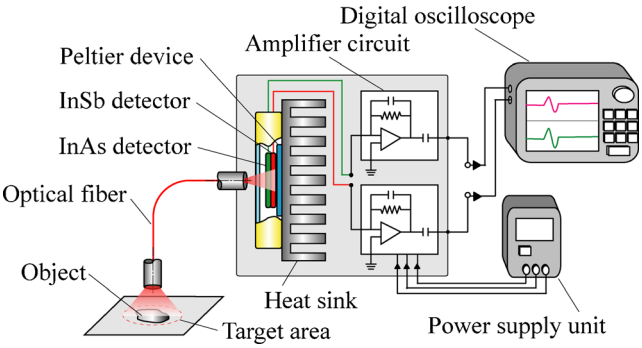

Fig. 5 Schematic illustration of two-color pyrometer with optical fiber

highest temperature in the temperature distribution at the cutting edge because the cutting speed was the maximum [16]. The tool temperature was measured when the corner edge of the outer insert reached a depth of 3.0 mm from the upper surface of the workpiece. The time for the corner edge of the outer insert to reach the measurement area of the optical fiber was calculated from the drilling start time, which was obtained from the dynamometer output and the feed speed of the drill.

2.4 Experimental procedure

An image of the experimental setup and the experimental conditions are shown in Fig. 7 and Table 1. The drilling tests were carried out using a vertical machining center. The workpiece was fixed on a dynamometer mounted on the table of the machining center to measure the thrust force. The output voltages from the two-color pyrometer and dynamometer were simultaneously saved by a digital oscilloscope. In the case of the solid drill, the tool temperature at the peripheral corner edge was measured using a method similar to that in the case of the indexable drill. Additionally, the translational force component occurred on the same plane as the torque component during drilling, when using the indexable drill, because it did not have an axisymmetric geometry. However, the dynamometer, which could measure the thrust force with the drill feed direction and cutting torque around the drill's rotational axis, was used. This type of dynamometer cannot measure the cutting torque caused by using an indexable drill. Thus, the thrust force was measured to examine the cutting force in this experiment. Moreover, it was confirmed that the thrust force of the solid drill showed the same tendency as the cutting torque in all of the workpiece materials used in this experiment. From Table 1, both drills were coated with the same PVD coating film, because the coating material had an influence on the tool temperature during cutting [13]. Low cutting speeds of 25 and 50 m/min were used to ensure uniform cutting conditions for all the materials, even though carbon steel and stainless steel can generally be drilled at higher speeds. This made it possible to observe the influence of the workpiece material properties on the cutting characteristics for both drills. The cutting characteristics of the drills were compared under the same feed rate f, but the feed per tooth values of the indexable and solid drills were different, because the material removal rates of the drills were uniform. An oil mist was constantly supplied from an oil hole at the bottom flank face of each drill. The drilling tests were carried out over two times for every cutting condition, and it was confirmed that their output waveforms obtained from the two-color pyrometer and dynamometer were comparable under same condition. Additionally, the corner edge temperature of the outer insert was calculated using the mean value of ten pulses for each cutting condition.

Fig. 4 Details of outer insert

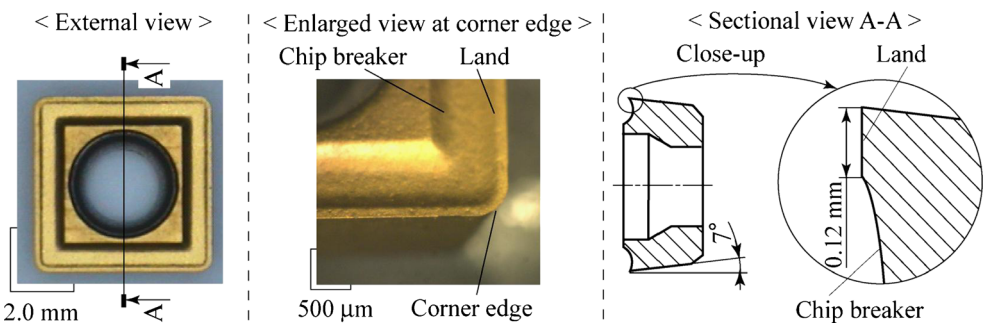

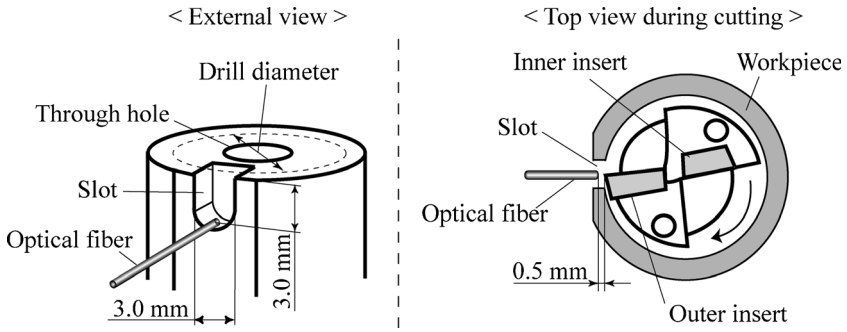

Fig. 6 Setup for tool temperature measurement

To evaluate the finished surface integrity, the inner-surface roughness Ra was measured. The surface roughness was the arithmetic mean roughness, which was measured in the drill feed direction using a stylus-type surface roughness meter and calculated using the mean value of three measurement parts. The cutoff wavelength and evaluation length were set at 0.8 and 4.0 mm, respectively.

The bottom flank wear of the outer insert was measured at the maximum wear width on the bottom flank face of the outer insert. In addition, cutting length was defined as the contact length between the workpiece and the peripheral corner edge of the outer insert and was calculated from the cutting time, tool diameter, and tool rotating speed.

2.5 Material properties of workpieces

AISI 1045 carbon steel (1045), AISI 304 austenitic stainless steel (304), titanium α+β alloy (Ti–6Al–4V/Ti64), and nickel-based alloy (Inconel 718/I718) were selected as the workpiece materials. The machinability can be mainly characterized by hardness, tensile strength, ultimate elongation, and thermal conductivity of the workpiece material. These properties are summarized in Table 2, along with a machinability rating (MR). These properties are mean values, which has been indicated in multiple publications and articles [17–20], because the material properties fluctuate to some degree according to factors such as the manufacturing process and heat treatment method. The material hardness values of the workpieces used in this experiment are also shown in Table 2, which shows that the measured hardness value was similar to the mean value for each material. Thus, it is clear that the mean values in Table 2 were reflected in the material properties of the workpieces used in this experiment. MR is defined as a percentage of the material removal rate and it was determined AISI B1112 carbon steel a MR of 100 % [21]. Table 2 shows that the properties of 304, Ti64, and I718 are very different, although they are classified as difficult-to-cut

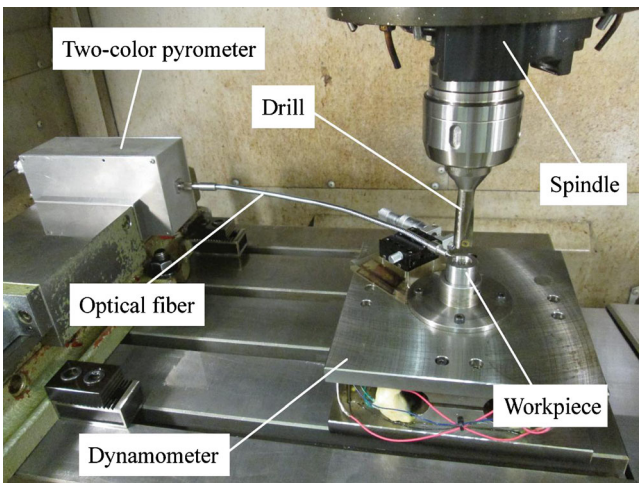

Fig. 7 Outline of experimental arrangement

Table 1 Experimental conditions

Drill	
Indexable	
(Ti,Al)N+TiN-coated carbide with two oil holes	
Rake angle	γ=0° (except for the chip breaker)
Relief angle	ζ=7° (outer insert) and 11° (inner insert)
Back taper angle	ξ=2.5°
Chamfer width	w_c=0.12 mm and Chamfer angle ψ_c=0°
Diameter	D=16 mm
Effective length	L_d=48 mm and 2 flutes
Solid	
(Ti,Al)N+TiN-coated carbide with two oil holes	
Point angle	2α=140°
Rake angle	γ=30° (on outer diameter)
Relief angle	ζ=10°
Back taper angle	ξ=0.15°
Chamfer width	w_c=0.1 mm and Chamfer angle ψ_c=10°
Diameter	D=16 mm
Effective length	L_d=39 mm and 2 flutes
Cutting speed	v_c=25, 50 m/min
Feed rate	f=0.05, 0.10 mm/rev
Prepared hole	Diameter D_p=5.0 and 11.0 mm
Lubrication	MQL (vegetable oil and water insoluble)
Supply pressure	p=0.5 MPa
Flow rate	q=6 and 44 ml/h

Table 2 Material properties of workpiece

Material	Vickers hardness (measured value; MPa)	Vickers hardness (MPa)	Tensile strength (MPa)	Ultimate elongation (%)	Thermal conductivity at 20 °C (W/m K)	Machinability rating (%)
1045	180	198	623	21	49	60
304	161	157	606	47	17	34
Ti64	304	318	1,026	12	8	22
I718	418	399	1,252	22	11	13

materials. The 304 had a high ultimate elongation, Ti64 had a low thermal conductivity, and I718 had a high hardness, a high tensile strength, and a low thermal conductivity.

3 Experimental results and discussion

3.1 Tool temperature at peripheral corner edge

Figure 8 shows a comparison of tool temperature θ_α for the indexable and solid drills when the four kinds of workpiece materials were cut at cutting speed v_c=25 m/min and feed rate f=0.10 mm/rev. The feed rate was the same for both drills in order to evaluate the cutting characteristics under the same material removal rate, whereas the feed per tooth of the solid drill was half that of the indexable drill. It is clear that θ_α increased remarkably in the order of 1045, 304, Ti64, and I718 for both drills. This tendency was analogous to the MR indicated in Table 2. However, it should be noted that there was a clear difference in the tendencies of the indexable and solid drills. In the case of Ti64 and I718, the θ_α value of the indexable drill was lower than that of the solid drill, whereas it was approximately 100 °C (or more) higher than that of the solid drill in cutting 1045 and 304. In particular, it can be said that the indexable drill could decrease the tool temperature compared with the solid drill when cutting I718. This difference in the θ_α values for the drills was reflected in the various differences in the drill geometry. The cutting edge length of the indexable drill in contact with the workpiece was shorter

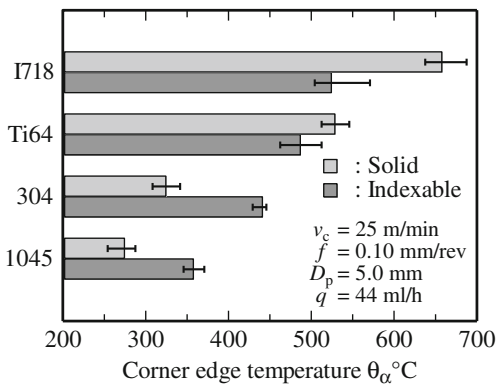

Fig. 8 Influence of workpiece material on tool temperature at corner edge

than that of the solid drill, because the two inserts shared the cutting area, as shown in Fig. 3, whereas the solid drill had two cutting edges, which covered the cutting area from the center to the peripheral corner. In addition, the point angle of the indexable drill was close to 180°°, whereas that of the solid drill was 140°. Therefore, the difference in the edge length in contact with the workpiece became more remarkable. In a case where the contact length between the cutting edge and workpiece was short, the energy required to cut into the workpiece decreased, and the heat generated during cutting became low. Moreover, in the case of the indexable drill, the contact area between the drill and workpiece, except for the bottom cutting edge, was smaller than that of the solid drill, because the indexable drill had a larger back taper angle and there was no margin on the side flank face. Consequently, the heat generated at the peripheral corner edge of the indexable drill was also lower than that of the solid drill because of the friction difference between the margin area of the drill and inner surface of the machined hole. Additionally, the indexable drill had a groove-type chip breaker on the rake face of the insert, and Shinozuka et al. [22] reported that a chip breaker could decrease the tool temperature because the contact area between the rake face of the cutting edge and the chip become small. Solid twist drills, which have a groove-type chip breaker on the rake face, have been developed and evaluated in numerous papers [23,24]. However, a solid drill with a groove-type chip breaker has not been widely used, because the cutting edge geometry of a solid drill changes during use as a result of the regrinding process needed for maintenance. Thus, the θ_α values of the indexable drill were lower than those of the solid drill only when cutting the Ti64 and I718 because of the high mechanical intensity and low thermal conductivity. Conversely, the θ_α values of the indexable drill were higher than those of the solid drill when cutting the 1045 and 304, which had relatively high MR value. This tendency seems to show that the influence of the feed per tooth on θ_α was stronger than that of the cutting edge length in contact with the workpiece because the workpiece hardness and thermal conductivity of 1045 were comparatively low and high, respectively. On the other hand, it is thought that the θ_α of 304, which has a relatively low thermal conductivity, was higher in the case of the indexable drill because of the influence of the thrust force, as described later.

3.2 Thrust force

Figure 9 shows the influence of the workpiece material on the thrust force F_t. The F_t of the solid drill increased in order of 1045, 304, Ti64, and I718, and it reached a maximum of approximately 1.7 kN. This tendency was analogous to tool temperature θ_α and the MR value, and it is thought that the F_t of the solid drill was influenced to a large degree by the mechanical intensity such as the hardness and tensile strength of the workpiece. On the other hand, the F_t values of the indexable drill were lower than those of the solid drill, except with 304. In particular, it was approximately 40 % of the value for the solid drill when cutting Ti64. With the indexable drill, the F_t value for Ti64, which has a high mechanical intensity, was even lower than that of 1045. It seems that this phenomenon was influenced by the ultimate elongation of the workpiece materials. On the other hand, in the cutting of 304, the tool temperature θ_α of the indexable drill was higher than that of the solid drill, as shown in the previous section, because the F_t of the indexable drill was higher than that of the solid drill.

A comparison of the cross-sectional images of the chips, which were embedded in resin, is presented in Fig. 10a, b in order to evaluate the chip morphologies for 304 and Ti64 when using the indexable drill. The cutting conditions were the same as those for the case shown in Fig. 9, and both cross-sectional images of chips were taken in the chip flow direction. From Fig. 10a, b, it can be seen that the chips showed similar saw-tooth-type chip formations. However, the thicknesses of the chips were clearly different, even with the same feed per tooth, with the 304 chip thickness larger than that of Ti64 for the indexable drill. Generally, the chip thickness increases when the shear angle decreases and the cutting force increases. Therefore, this seems to explain why 304 showed a high thrust force in the case of the indexable drill. Consequently, the indexable drill showed excellent performance from the viewpoint of the tool temperature and thrust force when cutting the workpiece material represented by Ti64, which has a high mechanical intensity, low thermal conductivity, and low ultimate elongation.

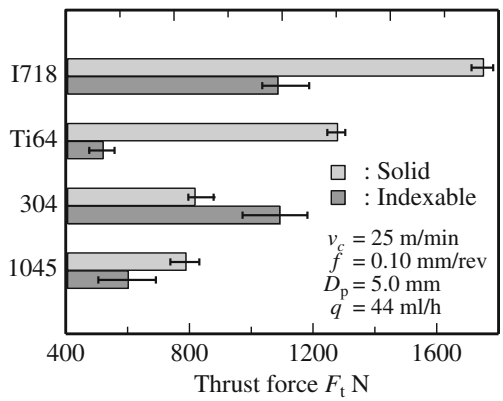

Fig. 9 Influence of workpiece material on thrust force

3.3 Influence of cutting speed and feed rate on cutting characteristics in titanium alloy

Figure 11a, b shows the tool temperature at the peripheral corner edge θ_α and thrust force F_t when cutting Ti64 (for which the indexable drill showed satisfactory performance) using both drills while varying the cutting speed v_c and feed per tooth f_z. The material removal rate were the same for all the cutting conditions except v_c=25 m/min and f_z=0.05 mm/tooth with indexable drill, and the material removal rate of this condition (v_c=25 m/min and f_z=0.05 mm/tooth with indexable drill) was a half that of the others. In the case of v_c=25 m/min and f_z=0.05 mm/tooth, the θ_α value of the indexable drill was approximately 70 °C lower than that of the solid drill. In this case, the feed per tooth was the same for the both drills. Therefore, this difference in θ_α was influenced by the cutting edge geometry, and it can also be said that the indexable drill was suitable for cutting Ti64, as previously mentioned. Additionally, slight increases in θ_α and F_t with an increase in the feed per tooth for f_z=0.05–0.10 mm/tooth were obtained with the indexable drill. By contrast, the influence of v_c on θ_α was clearly established and θ_α increased by 120 °C for v_c=25–50 m/min. Therefore, θ_α could be kept low using the cutting conditions with a low cutting speed and high feed rates when cutting Ti64 with an indexable drill, whereas θ_α became higher when using a low cutting speed and high feed rate for cutting 1045 [7]. Consequently, the optimum cutting conditions were changed by the properties of the workpiece material for the indexable drill, and the low-speed, high-feed-rate cutting was effective from the viewpoint of reducing the increase in θ_α when cutting a workpiece such as Ti64.

3.4 Inner-surface roughness

The roughness at the inner surface of drilled hole Ra in each workpiece material is shown in Fig. 12. The surface roughness values of the three difficult-to-cut materials cut with the indexable drill were relatively low and the same degree as when the solid drill was used for each material, whereas a clear difference was observed when cutting 1045. Okada et al. [7] reported that the surface roughness of 1045 cut with an indexable drill was improved remarkably as a result of the disappearance of the built-up edge under the high-speed cutting, and the inner-surface roughness had the same degree as with the solid drill. Conversely, the Ra value for the solid drill in the 1045 cutting was low, even for low-speed cutting. The solid drill had a margin area on the peripheral flank face, and this margin area was effective in improving the roughness of the inner surface. On the other hand, the indexable drill did not have a margin area on the peripheral flank face, and had a higher back taper angle and relief angle. Thus, the solid drill showed better surface roughness when cutting 1045,

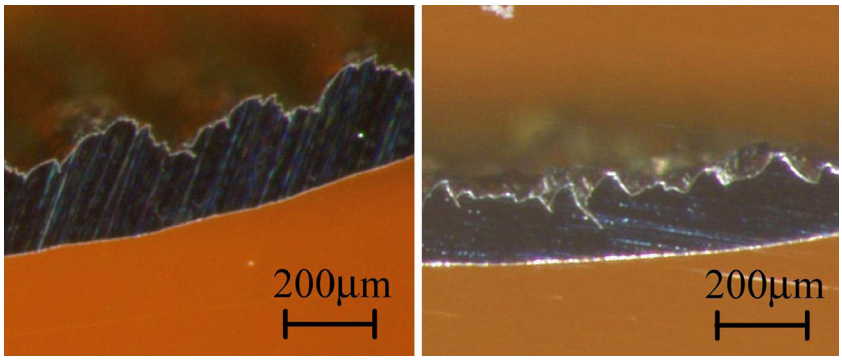

Fig. 10 Cross-sectional images of chips of 304 and Ti64 cut with indexable drill: **a** 304 and **b** Ti64

even for the condition where a built-up edge was generated. Moreover, in the case of the difficult-to-cut materials, when the cutting temperature became high and no built-up edge was generated, a lower roughness could be obtained by the indexable drill, as well as the solid drill.

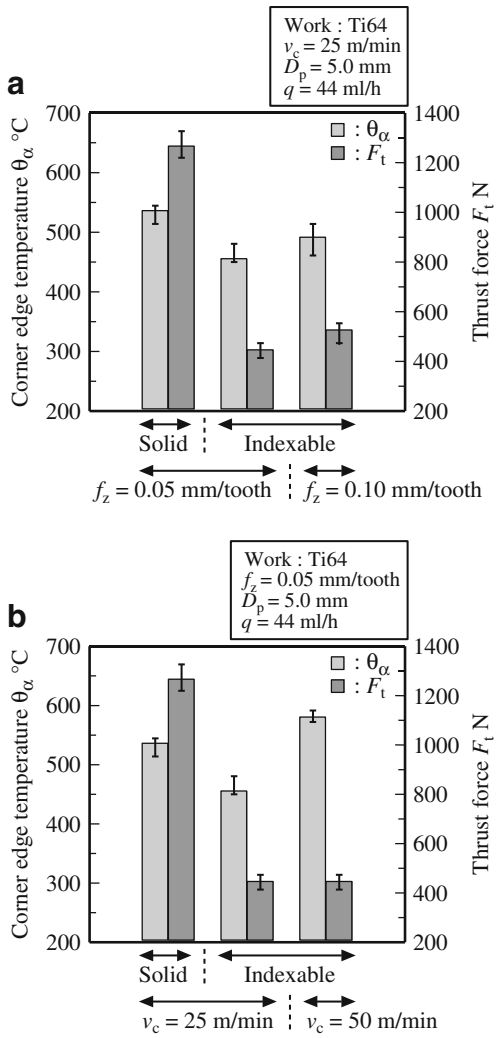

Fig. 11 Influence of cutting condition on tool flank temperature and thrust force: **a** v_c variation and **b** f_z variation

3.5 Behavior of cutting edge wear in cutting of 304

A tool wear test was performed to examine the wear behavior of the indexable drill. Figure 13 shows the relationship between cutting length L_c and the bottom flank wear of the outer insert VB_o. The indexable drill was used as the tool, and 304 was used as the workpiece material, which indicated a relatively high tool temperature and thrust force for the indexable drill. Oil mist flow rates of q=6 and 44 ml/h were used as the lubrication conditions because chipping was immediately caused with dry cutting even with a new tool. The depth of the drilled hole was 15 mm, and it was a blind hole. The prepared hole diameter was D_p=11 mm to eliminate the influence of the inner insert and focus on the wear behavior of the outer insert. From Fig. 13, the flank wear increased drastically at L_c=50.3 m for q=6 ml/h because of the occurrence of chipping. On the other hand, the wear width increased gradually after an initial wear of approximately VB_o=50 μm for q=44 ml/h, and no chipping was observed until L_c= 1,523 m. Under the two conditions, q=6 and 44 ml/h, VB_o was approximately 50 and 90 μm before chipping occurred, respectively, which was not very large. Therefore, it can be said that the tool life was determined by the occurrence of chipping under this condition, and the flow rate of the oil mist was an important factor for tool wear in the indexable drill.

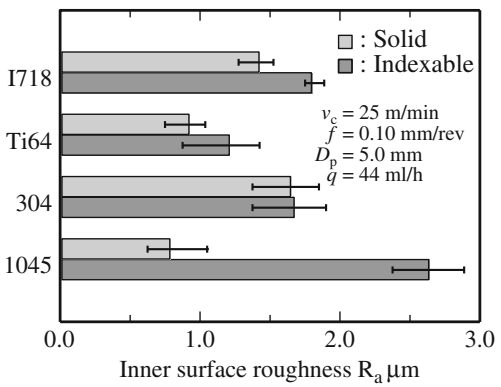

Fig. 12 Influence of workpiece material on inner-surface roughness

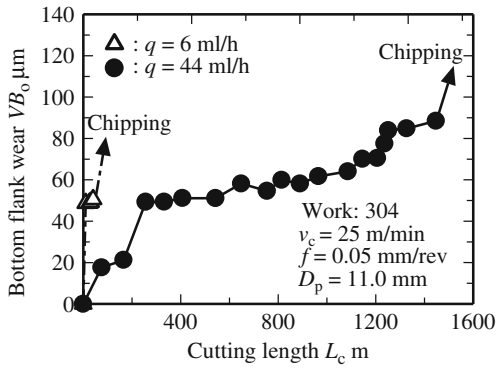

Fig. 13 Relationship between cutting length and bottom flank wear

Incidentally, chipping was occurred under these cutting conditions in two separate tool wear tests, and the clear difference between q=6 and 44 ml/h was confirmed in each test. Figure 14a, b shows the rake face and bottom flank face at the peripheral corner edge at each cutting length. In the case of q=6 ml/h, the flaking of the coating film can be clearly observed on the rake face at L_c=10.1 m, and it drastically increases to a large area from the cutting edge to the chip breaker at L_c=40.2 m. On the other hand, in the case of q=44 ml/h, the flaking of the coating film was slight, even at L_c=166 m, and the coating film can be observed on the chip breaker at L_c=1,327 m. This difference between q=6 and 44 ml/h seemed to be explained by the influence of the quantity of oil mist intervening between the rake face of the insert and the chip. The mechanical and thermal damages to the cutting edge caused by the abrasive effect were heavy when little oil mist was supplied. Thus, the flaking of the coating film at q=6 ml/h was observed at an early stage, because the coating film was subjected to the abrasive effect under the high-temperature environment. Consequently, it can be said that the flaking of the coating film and the abrasive wear of the base material mainly occur at the rake face, including the cutting edge and chip breaker, as a result of the abrasion between the rake face and the chips, and no remarkable wear was observed on the bottom flank face. This tendency seems to be explained by the low rake angle and high back taper angle of the indexable drill, as shown in Table 1. In general, the wear behavior of the solid drill was mainly observed at the flank face [25]. Thus, there is clearly a difference between the wear behaviors of the indexable and solid drills. Figure 15a, b shows the SEM images of the worn outer insert after chipping. These images are backscattered electron images (BEI), which can estimate the composition of an object by the graduations of color, with the color gradually becoming lighter with an increase in the atomic number of the composition. In the case of q=6 ml/h, clear chipping, which spread from the ridgeline of the cutting edge to the chip breaker, was observed, and the white area was clear at the rake face, whereas almost the entire area showed a dark gray color at q=44 ml/h. These white and dark gray regions show

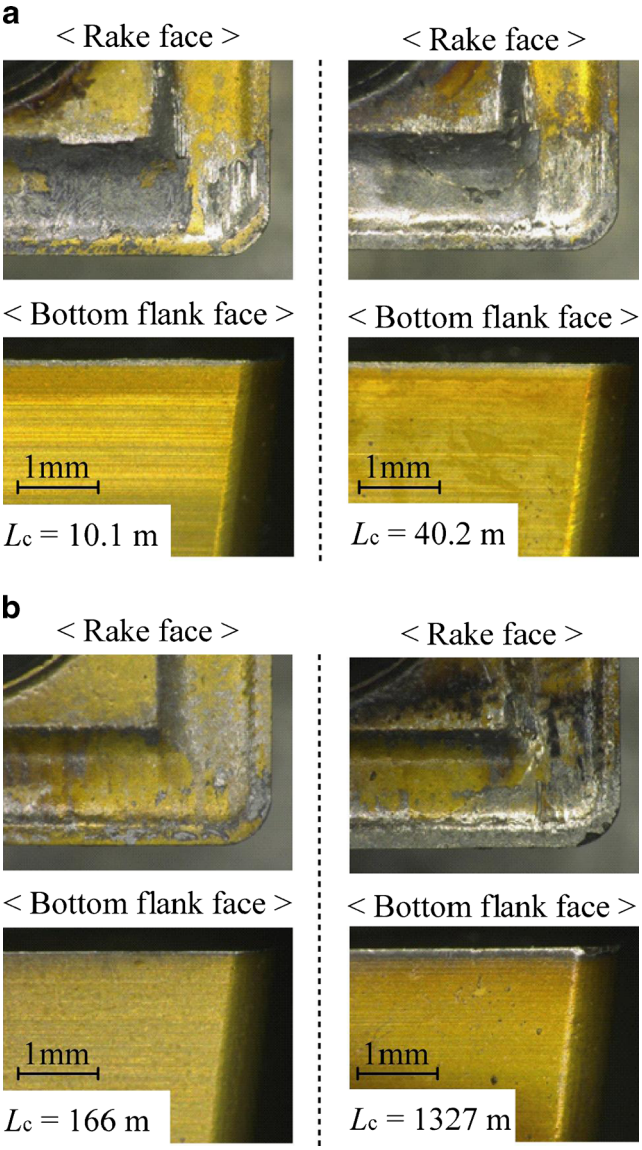

Fig. 14 Wear behavior around peripheral corner edge of outer insert. **a** Flow rate, q=6 ml/h. **b** Flow rate, q=44 ml/h

the flaking and coating film regions respectively. Additionally, the adhesion of the workpiece material to the rake face can be observed at q=6 ml/h. These results show that it is important to suppress the flaking of the coating film around the cutting

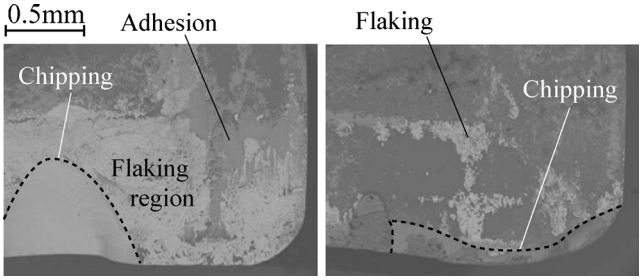

Fig. 15 SEM images around rake face at peripheral corner edge: **a** q=6 ml/h (L_c=50.3 m) and **b** q=44 ml/h (L_c=1,523 m)

edge and chip breaker and assure appropriate lubricant conditions to obtain a long tool life of the indexable drill. In particular, adhesive wear results from the flaking of the coating, which leads to chipping at the cutting edge and chip breaker.

4 Conclusions

To clarify the cutting performance of an indexable insert drill when cutting difficult-to-cut materials such as stainless steel, titanium alloy, and nickel-based alloy, the influence of the workpiece material and cutting condition on the tool temperature, thrust force, inner-surface roughness, and wear behavior were experimentally investigated in comparison with that of a solid-type twist drill, and the results were discussed. These results can be summarized as follows:

1. The tool temperature at the peripheral corner edge increased in the order of 1045, 304, Ti64, and I718 in the cases of the indexable and solid drills. The tool temperatures when cutting Ti64 and I718 with the indexable drill were lower than those of the solid drill, whereas the tool temperatures of the indexable drill were higher than those of the solid drill for cutting 1045 and 304.
2. The thrust forces of the indexable drill were lower than those of the solid drill, except for the case of 304 cutting. In particular, the indexable drill could cut the Ti64 using only 40 % of the thrust force needed in the case of the solid drill under the same cutting conditions.
3. When cutting Ti64 with the indexable drill, the influence of the cutting speed on the tool temperature was larger than that of the feed rate. Thus, cutting at a low speed and high feed rate could suppress the heat generation.
4. In the cutting of difficult-to-cut materials, no significant differences were observed in the inner-surface roughness values of the holes finished by the indexable and solid drills.
5. The flaking of the coating film on the rake face around the cutting edge and chip breaker occurred under a low-flow-rate condition for the oil mist in the cutting of 304. Adhesion of the workpiece material was also observed on the rake face.
6. The indexable drill, which is a small contact area between cutting edge and workpiece instead of having high feed per tooth than that of the solid drill, could cut under a lower tool temperature and thrust force than the solid drill for workpiece materials that had higher mechanical intensity, lower ultimate elongation, and lower thermal conductivity properties, such as Ti64 and I718.

Acknowledgments The authors gratefully acknowledge the financial support for this study by the Machine Tool Engineering Foundation.

References

1. Neugebauer R, Stoll A (2003) Ultrasonic application in drilling. J Mater Process Technol 149:633–639. doi:10.1016/j.jmatprotec.2003.10.062
2. Lazar M-B, Xirouchakis P (2013) Mechanical load distribution along the main cutting edges in drilling. J Mater Process Technol 213:245–260. doi:10.1016/j.jmatprotec.2012.09.020
3. Audy J (2008) A study of computer assisted analysis of effects of drill geometry and surface coating on forces and power in drilling. J Mater Process Technol 204:130–138. doi:10.1016/j.jmatprotec.2007.10.079
4. Lin T-R (2002) Cutting behavior of a TiN-coated carbide drill with curved cutting edges during high-speed machining of stainless steel. J Mater Process Technol 127:8–16
5. Tsao CC, Hocheng H (2008) Effects of peripheral drilling moment on delamination using special drill bits. J Mater Process Technol 201:471–476. doi:10.1016/j.jmatprotec.2007.11.225
6. Zhao H, Ehmann KF (2002) Development and performance analysis of new spade bit design. Int J Mach Tools Manuf 42:1403–1414
7. Okada M, Ueda T, Hosokawa A, M'Saoubi R, Muranaka T (2010) Cutting characteristics of indexable insert drill. Proc 4th CIRP Int Conf High Perform Cut 24–26 October, Gifu, Japan: 333–336
8. Venkatesh VC, Xue W (1996) A study of the built-up edge in drilling with indexable coated carbide inserts. J Mater Process Technol 58:379–384
9. Venkatesh VC, Xue W, Quinto DT (1992) Surface studies during indexable drilling with coated carbides of different geometry. CIRP Ann 41:613–616
10. Wang S, Venkatesh VC, Xue W (1991) A study on modification of endrills for finishing holes. J Mater Process Technol 28:83–92
11. Li R, Shih JA (2007) Spiral point drill temperature and stress in high-throughput drilling of titanium. Int J Mach Tools Manuf 47:2005–2017. doi:10.1016/j.ijmachtools.2007.01.014
12. Zeilmann RP, Weingaerther WL (2006) Analysis of temperature during of Ti6Al4V with minimal quantity of lubricant. J Mater Process Technol 179:124–127. doi:10.1016/j.jmatprotec.2006.03.077
13. Okada M, Hosokawa A, Tanaka R, Ueda T (2011) Cutting performance of PVD-coatedcarbide and CBN tools in hardmilling. Int J Mach Tools Manuf 51:127–132. doi:10.1016/j.ijmachtools.2010.10.007
14. Hosokawa A, Ueda T, Onishi R, Tanaka R, Furumoto T (2010) Turning of difficult-to machine materials with actively driven rotary tool. CIRP Ann 59:89–92. doi:10.1016/j.cirp.2010.03.053
15. Ueda T, Sato M, Hosokawa A, Ozawa M (2008) Development of infrared radiation pyrometer with optical fibers—two-color pyrometer with non-contact fiber coupler. CIRP Ann 57:69–72. doi:10.1016/j.cirp.2008.03.056
16. Ueda T, Nozaki R, Hosokawa A (2007) Temperature measurement of cutting edge in drilling-effect of oil mist. CIRP Ann 56:93–96. doi:10.1016/j.cirp.2007.05.024
17. Hoyt SL (1954) ASME handbook, metals properties. Mcgraw-Hill Book 58:162–163
18. Editorial Committee for Practical Metallic Materials Handbook (1962) Practical metallic materials handbook. Nikkan Kogyo Shimbun, Ltd.: 283–425 (in Japanese)
19. Hashiguti R (1958) Metallography handbook. Asakura Publishing Co., Ltd.: 595–666 (in Japanese)
20. The Japan Institute of Metals and Materials (1974) Iron materials handbook. Maruzen Company, Ltd.: 534–666 (in Japanese)
21. Jin LZ, Sandström R (1994) Machinability data applied to materials selection. Mater Des 15:339–346

22. Shinozuka J, Obikawa T, Shirakashi T (1996) Chip breaking analysis from the viewpoint of the optimum cutting tool geometry design. J Mater Process Technol 62:345–351
23. Sushanta K, Sahu O, Ozdoganlar B, DeVor RE, Kapoor SG (2003) Effect of groove-type chip breakers on twist drill performance. Int J Mach Tools Manuf 43:617–627. doi:10.1016/S0890-6955(02)00303-6
24. Degenhardt JA, DeVor RE, Kapoor SG (2005) Generalized groove-type chip breaker effects on drilling for different drill diameters and flute shapes. Int J Mach Tools Manuf 45:1588–1597. doi:10.1016/j.ijmachtools.2005.02.009
25. Chen W-C, Liu X-D (2000) Study on the various coated twist drills for stainless steels drilling. J Mater Process Technol 99:226–230